SSCL-343

Superconducting Super Collider Laboratory

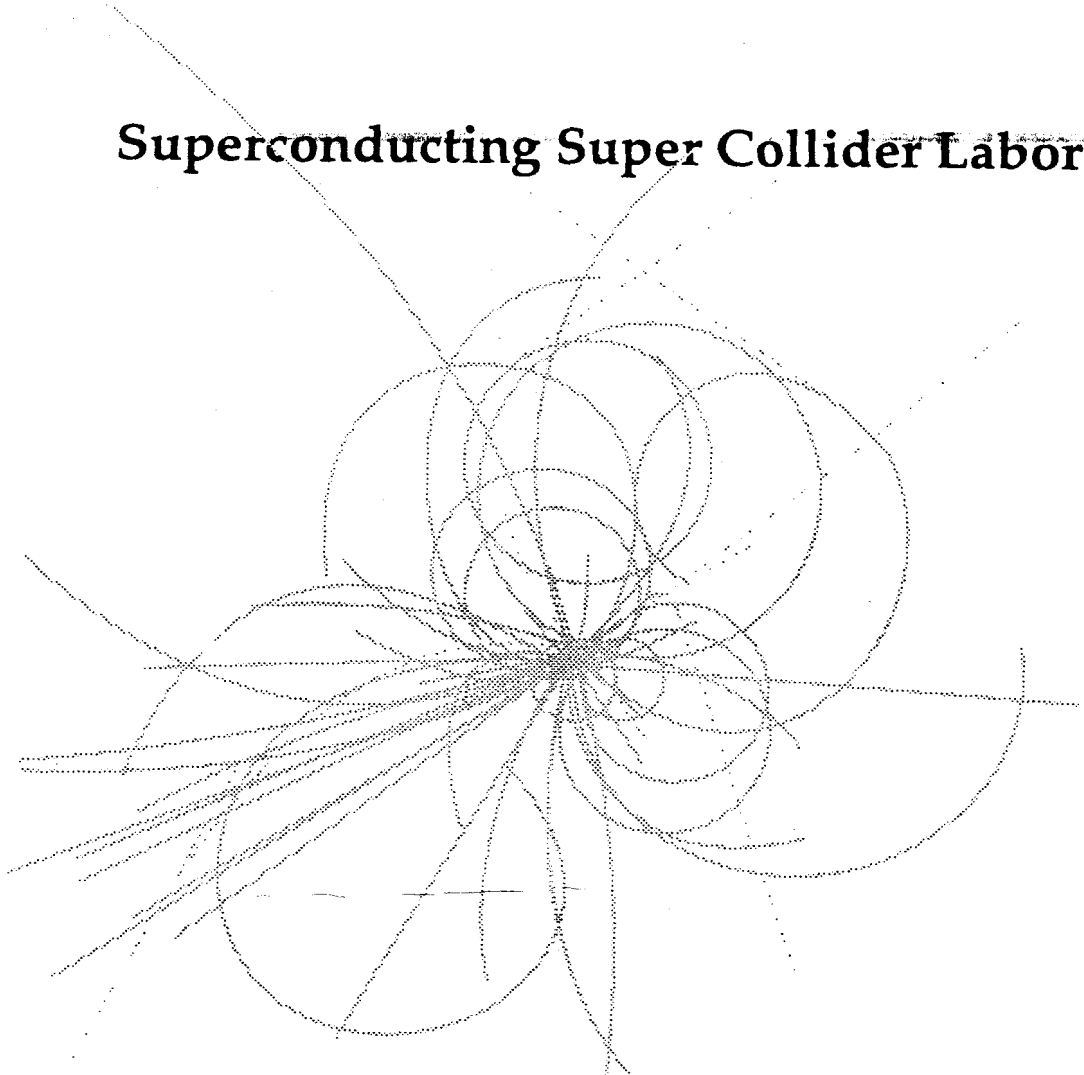

A Controlled Master Frequency Oscillator for the SSC Low Energy Booster

L. K. Mestha

January 1991

SSCL–343

A CONTROLLED MASTER FREQUENCY OSCILLATOR FOR THE SSC LOW ENERGY BOOSTER

L.K. Mestha

Superconducting Super Collider Laboratory*
2550 Beckleymeade Avenue
Dallas, TX 75237

January 1991

* Operated by the Universities Research Association, Inc., for the U.S. Department of Energy under Contract No. DE-AC02-89ER40486.

SSCL–343

A CONTROLLED MASTER FREQUENCY OSCILLATOR FOR THE SSC LOW ENERGY BOOSTER

L.K. Mestha

Superconducting Super Collider Laboratory*
2550 Beckleymeade Avenue
Dallas, TX 75237

January 1991

Abstract

A variable frequency oscillator is normally used to generate the master frequency for an accelerator. For the Low Energy Booster (LEB) at the Superconducting Super Collider (SSC) the prospects of using a Direct Digital Synthesizer (DDS) to vary the frequency from 47 MHz to 59 MHz are considered. A Digital Signal Processor (DSP) which can be loaded with the desired frequency values is interfaced to the DDS. These values are launched on the DDS at known intervals to ramp the frequency smoothly. In this paper the observations made while ramping the frequency are discussed. The design principle of the digital synchronization of the LEB frequency source with the Medium Energy Booster (MEB) frequency source is also briefly discussed. When developed, such a system can be used to synchronize the two machines.

* Operated by the Universities Research Association, Inc., for the U.S. Department of Energy under Contract No. DE-AC02-89ER40486.

1. INTRODUCTION

In this paper, a scheme for generating a controlled accelerating frequency for the Superconducting Super Collider (SSC) Low Energy Booster (LEB) is outlined. The fully developed system will be capable of delivering the sinusoidal low-level rf signal with feedback paths to synchronize the LEB and Medium Energy Booster (MEB) frequency sources by controlling the phase (not just the frequency) of the LEB throughout the LEB acceleration. This will help in extracting the beam from the LEB at a known MEB turn. The hardware to establish the "proof of principle" is described.

2. MASTER FREQUENCY

It is well known that the desired master frequency can be obtained from the following relationship when the magnetic field profile is known with respect to time:[1-3]

$$f = \frac{ch}{C\sqrt{1 + \left[\frac{(mc^2)/e}{\rho c B(t)}\right]^2}} \tag{1}$$

Where,

c = Speed of light

h = Harmonic number

C = Path length of the synchronous orbit

m = Mass of the particle

e = Charge on the particle

ρ = Effective bending radius

B = Magnetic field strength.

For the LEB the frequency curve is shown in Figure 1. The LEB cycle has a frequency of 10 Hz and the momentum has a pure sine-wave dependency with the LEB cycle frequency. The injection and extraction momenta are 1.219 GeV/c and 12 GeV/c, respectively. The corresponding magnetic fields are 0.12157 Tesla and 1.1968 Tesla.[3] For these parameters the LEB rf sweeps between 47.518 MHz and 59.776 MHz. It is clear from the df/dt curve in Figure 1 that a maximum rate of change of frequency of 1036.8 MHz/sec takes place at about 5.7 ms into the LEB cycle. A digital system should be able to follow the ramp rate without producing large frequency steps that would cause unwanted beam excursions. A sampling interval of about a microsecond is thought to be adequate; the system under development will be capable of stepping as fast as an 0.18 μsec interval. This means the highest step in the revolution frequency will be 1.728 Hz (assuming a harmonic number of 108).

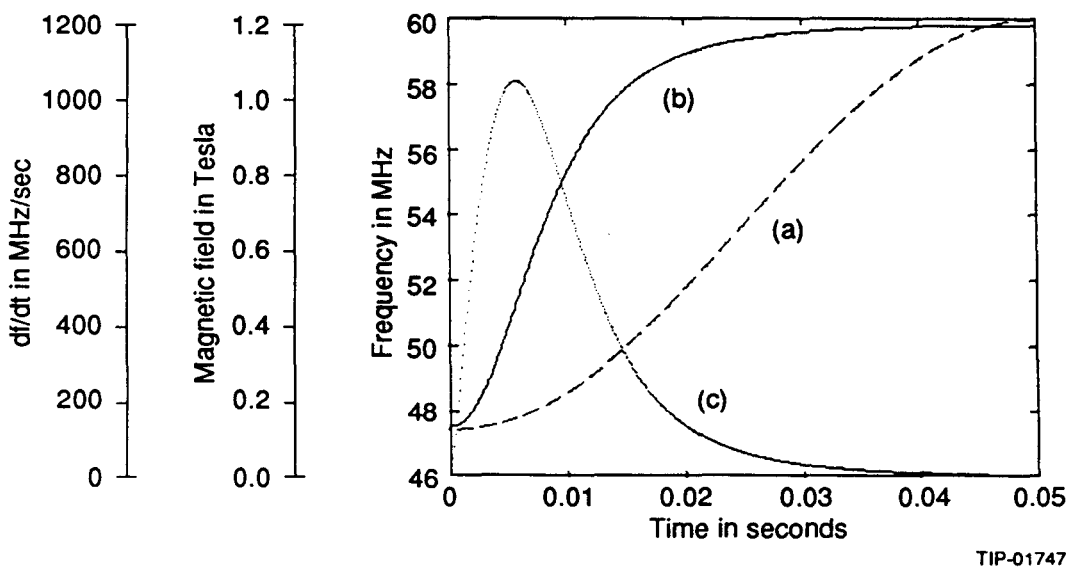

Figure 1. (a) Magnetic field, (b) Frequency, and (c) Rate of change of frequency as a function of time.

3. SYNCHRONIZATION PRINCIPLE

When the field ramps up in the LEB, acceleration of the beam occurs. As the extraction time nears, the phase of the LEB rf must be adjusted to match the phase of the next accelerator—in this case the MEB. During transfer the MEB rf is essentially running exactly at the LEB extraction frequency. In the literature one can see two schemes for achieving synchronous transfer of bunched beams from one accelerator to the other,[4–12] namely the phase-locking and the phase-slippage schemes. In the phase-locking scheme, at a known time before injection to the next accelerator, the phase and frequencies of the accelerating machine are locked to the extraction frequency. The time required to phase-lock the two frequencies depends on the lattice parameters of the accelerating machine.[1,3] In the phase-slippage scheme, at a predetermined time before transfer, the frequency of the accelerating machine is offset a few cycles relative to the extraction frequency. The phase of the accelerating frequency slips relative to the fixed frequency, resulting in several phase coincidence points of the reference wave which occur at a beat frequency equal to the offset frequency. One of them is used to trigger the synchronous transfer of the beam.

A more general approach for synchronization is to consider the "locking" of the phase of the variable frequency source with the phase of the extraction frequency source throughout the acceleration. Since this approach consists of maintaining control of the phase with a suitable feedback mechanism, it would be more appropriate to call it a "phase-control" scheme. In this scheme the rf wave (also called the reference rf wave) is forced to follow a pre-programmed "trip-plan" so that at the instant of transfer it will have the same phase as the MEB rf wave (except for constant phase offset). The feedback loop corrects for any deviation from the trip-plan. The trip-plan has at least one point at flat B-field region where the machines have exact phase for the purpose of synchronous beam transfer. With this scheme it is possible to synchronize two rf sources starting from a random phase difference.

When there is no error in the field, we can calculate the time at which the two reference rf waves match for beam transfer. Field deviations invalidate the calculation. The phase of the LEB reference rf wave from a given time during acceleration is equal to

$$\Psi_{\mathrm{LEB}} = \frac{2\pi}{h} \int_0^{\tau} R f(t) dt \tag{2}$$

Similarly the phase of the MEB reference rf wave can be written as:

$$\Psi_{\mathrm{MEB}} = \frac{2\pi R'}{h'} f' \tau \tag{3}$$

The notations R and R', the radii of the orbits, f and f', the rf frequencies, and h and h', the harmonic numbers of the LEB and the MEB, are used; τ is the time interval over which the integration is carried out. The difference in Equations 2 and 3 is the "synchronizing phase," Ψ. That is,

$$\Psi = |\Psi_{\mathrm{MEB}} - \Psi_{\mathrm{LEB}}| \tag{4}$$

For synchronous transfer, the synchronizing phase is equal to zero (ignoring the transfer line delays). Since the present discussion concerns two circular machines with non-integer circumference ratios (22/3), the LEB reference rf wave would have completed several full turns and a semi-turn at the end of one MEB turn. If the two frequencies are the same, then the LEB reference rf wave completes 7 full turns and a semi-turn equal to one-third the LEB circumference, which is the case with flat B-field. The semi-turn is not one-third the circumference ratio when the frequencies are different. Equation 4 is plotted in Figure 2 for each MEB turn. The '+' marks represent the position of the LEB reference rf wave for each MEB turn away from the transfer point. The phase values are shown from 0 to 540 meters to cover the full circumference of the LEB. Path length representing full turns completed by the LEB reference wave is ignored, since it is of no significance for synchronization. In Figure 3 the positions of two rf

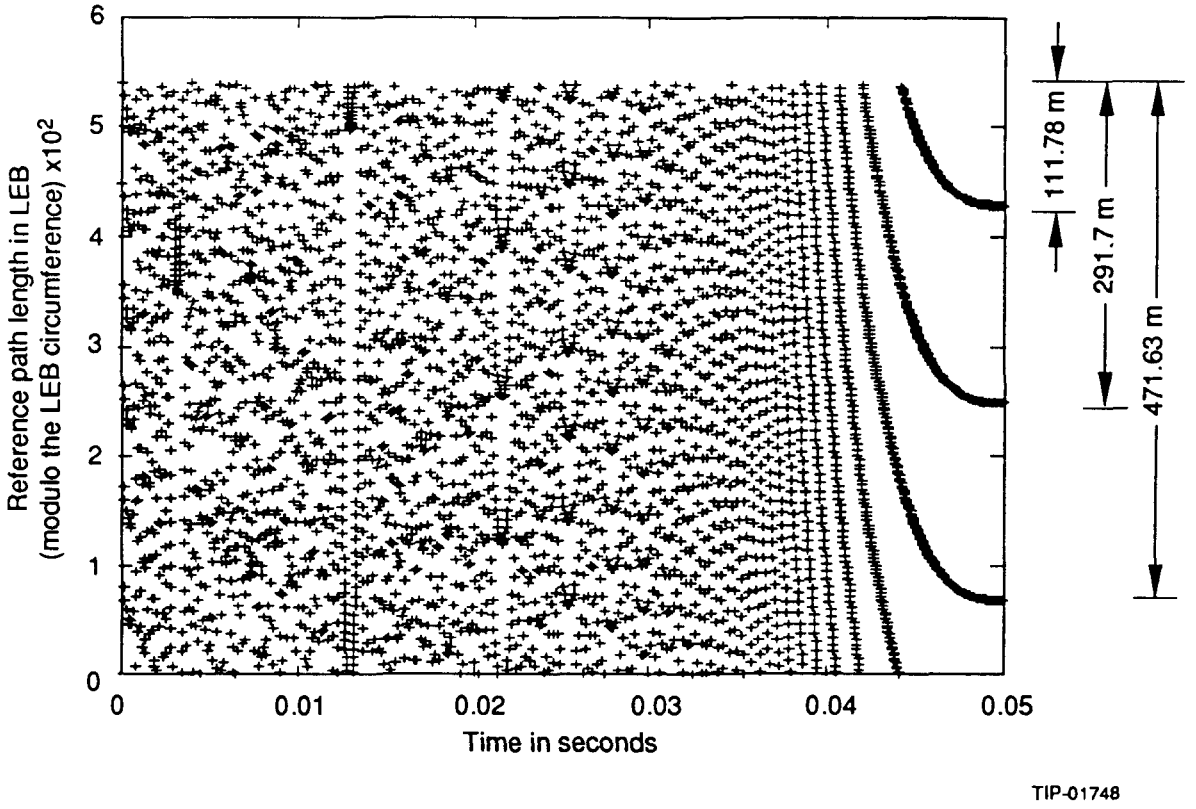

Figure 2. Synchronizing phase during acceleration in the LEB (phase not adjusted).

reference waves are shown for the first four turns followed by the last four turns of the MEB. The transfer line delays are ignored for simplicity. In Figure 2 three curves approach constancy at 50 msec; this is due to the fraction "1/3" in the circumference ratio. The decay is due to the fact that the difference in frequencies is narrowing as the time approaches the transfer time, when the magnetic field is at its maximum. In this region every third point is on the same curve. This means the relative phasing between the two reference waves is constant every time the MEB reference wave completes three turns. This is clear from Figure 3 when comparing turn numbers 3771 and 3774.

The synchronizing phase as seen from Figures 2 and 3 is not zero for transfer purposes. Also, if the LEB reference wave is controlled to the trip-plan shown in Figure 2, there may be synchronization with the MEB reference wave, but transfer cannot be matched. Instead, if the trip-plan is offset by 111.78 meters right at the beginning and an arbitrary rf wave is arranged to follow the new

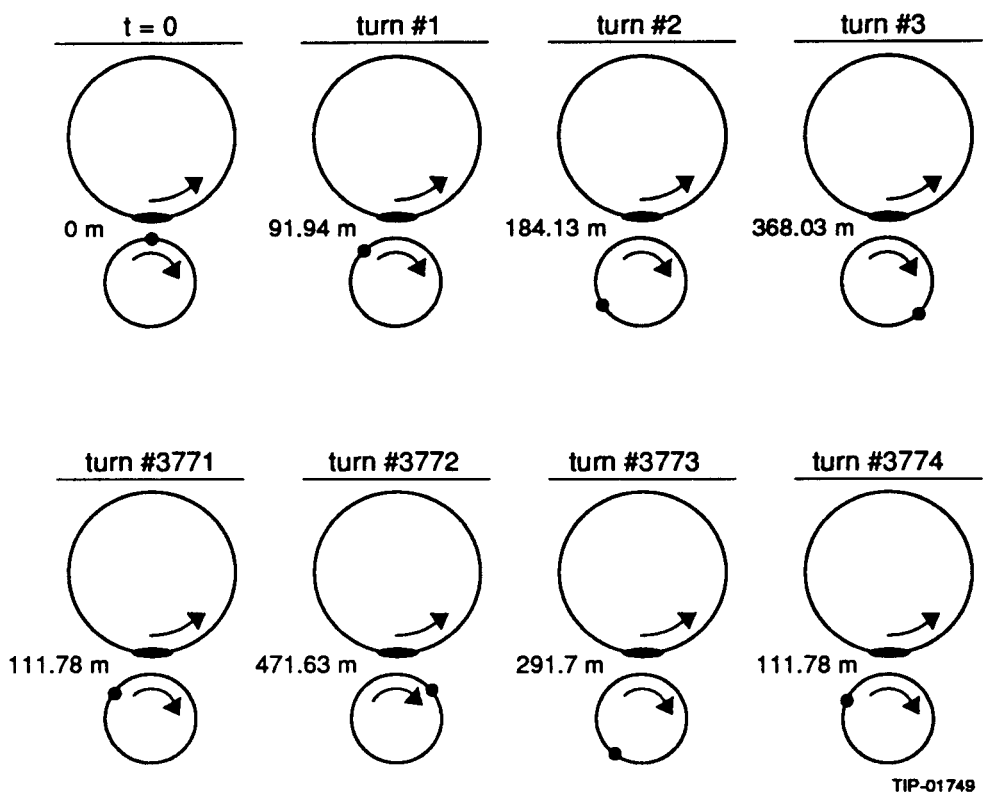

Figure 3. Position of the LEB reference wave for the first and the last four MEB turns (phase not adjusted). Positions are for the synchronizing phase shown in Figure 2. Numbers with extension 'm' represent the path length to be completed by the LEB reference rf wave to reach the transfer point after each MEB turn.

synchronizing phase, then there will be several transfer points. The new trip-plan is shown in Figure 4. Figure 5 is the same as Figure 3, but with the new LEB phase of Figure 4. From Figure 5 it is clear that the turn numbers 3771 and 3774 have zero phase.

4. SYSTEM MODEL

The system model can be obtained by introducing error terms for the beam orbit and the frequency in Equation 2. Let $\delta R(t)$ be the deviation in the radius of the orbit and $\delta f(t)$ be the error in the master frequency. The phase equation becomes:

$$\Psi'(t) = \frac{2\pi}{h} \int (R + \delta R(t))(f(t) + \delta f(t))dt \tag{5}$$

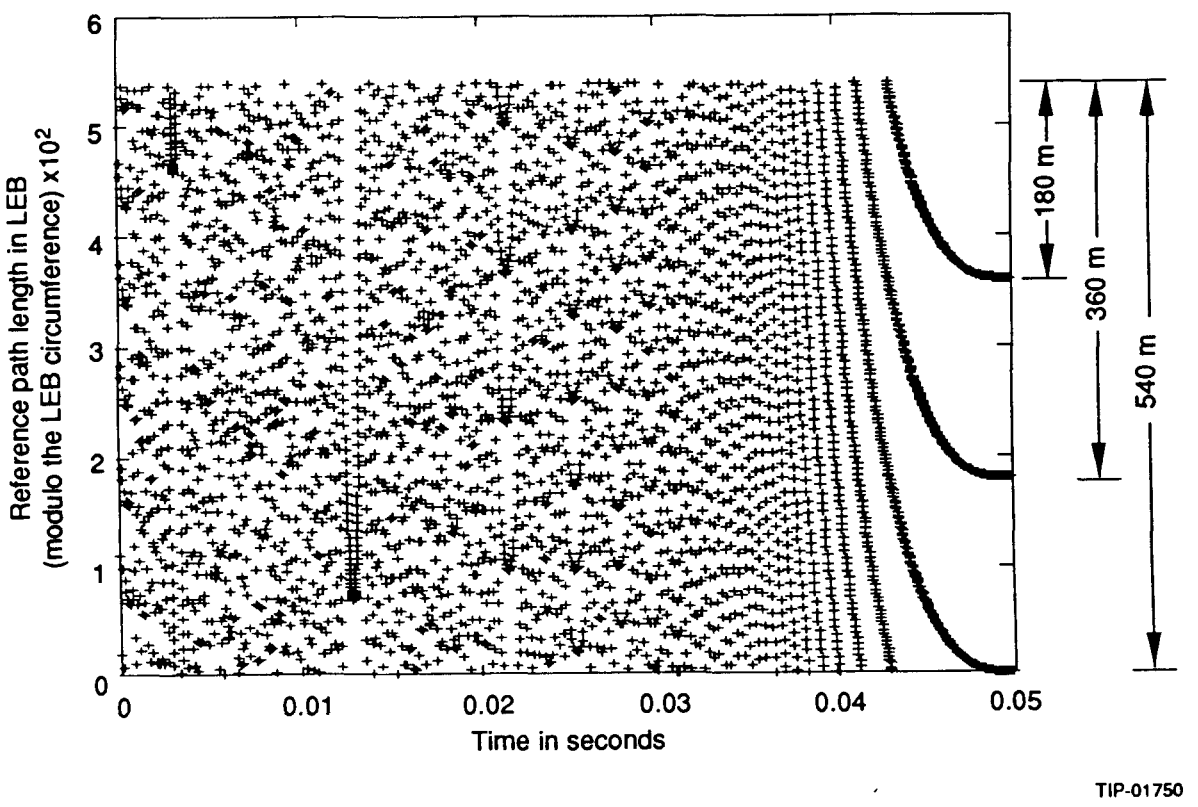

Figure 4. LEB Trip-Plan (phase adjusted to zero at transfer time).

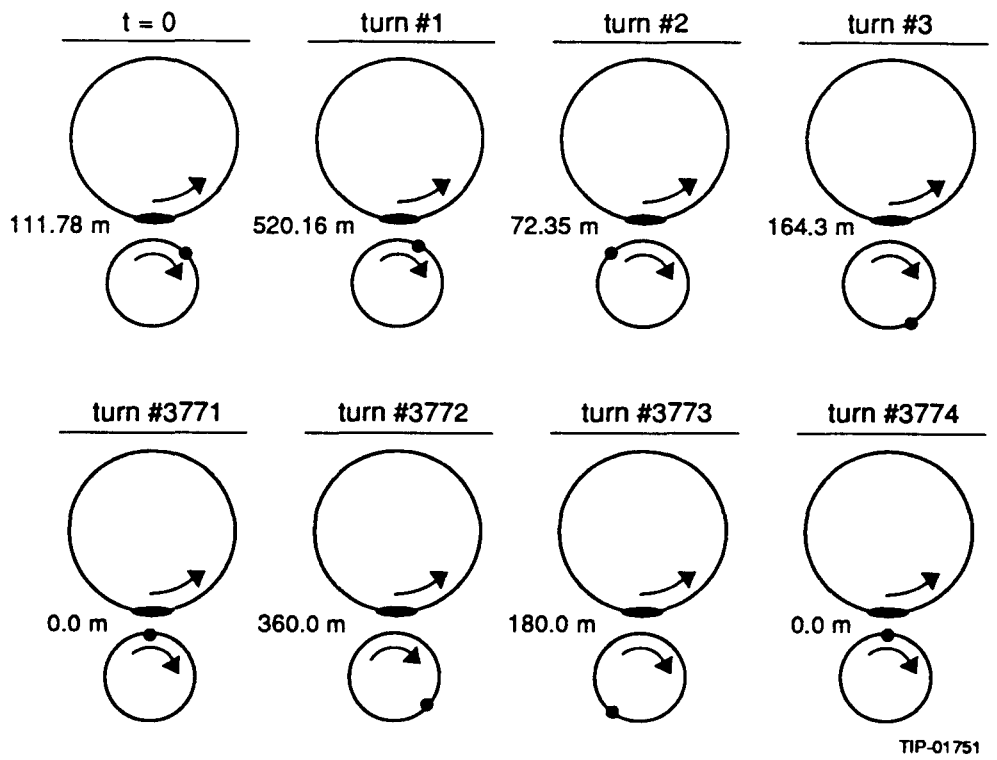

Figure 5. Position of the LEB reference wave for first and last four MEB turns (phase adjusted to zero at transfer time, 3774th turn).

The sign of $\delta R(t)$ depends on which side of transition the machine is operating. Since the control philosophy is to maintain the trip-plan shown in Figure 4 by modulating the LEB frequency, an equation for the error in synchronizing phase in terms of the frequency is required. This phase error is equal to the offset in the path length covered by the LEB reference wave from the ideal path. Hence it is given by:

$$\delta\Psi(t) = \Psi'(t) - \Psi_{\mathrm{LEB}}(t) \tag{6}$$

Substituting Equations 2 and 5 in Equation 6 and taking the first derivative with respect to time, the following differential equation is obtained.

$$\frac{d\delta\Psi(t)}{dt} = \frac{2\pi}{h}(\delta R(t)f(t) + R\delta f(t) + \delta R(t)\delta f(t)) \tag{7}$$

In Equation 7, in the absence of B-field error (i.e., $\delta B(t) = 0$), $\delta R(t)$ can be related to frequency in the usual way as follows.[13]

$$\frac{\delta f(t)}{f(t)} = -\frac{\delta R(t)}{R}\left[1 - \frac{\gamma_T^2}{\gamma^2(t)}\right] \tag{8}$$

where $\gamma(t)$ is a function of frequency. Substituting for $\delta R(t)$ from Equation 8 in Equation 7, a first order non-linear differential equation is obtained.

$$\frac{d\delta\Psi(t)}{dt} = \frac{2\pi R}{h}\left[\frac{\gamma_T^2}{\gamma_T^2 - \gamma^2(t)}\right]\delta f(t) + \frac{2\pi R}{hf(t)}\left[\frac{\gamma^2}{\gamma_T^2 - \gamma^2(t)}\right]\delta f^2(t) \tag{9}$$

Equation 9 shows that the first term is time-dependent due to the ramping in frequency. The second-order terms are due to the errors in the radial position. If the phase error is known, then a feedback loop can be arranged to maintain $\delta\Psi(t)$ near zero.

A scheme to calculate the phase error by measuring the LEB phase is described below. With this quantity known, it is clearly possible to set up a feedback control loop which can modulate the LEB frequency to reduce the error. A feedback controller based on Sliding-Mode techniques which accommodates the time-varying nature of the system is being considered. Since the loop gain of such a system is infinite, the system is not susceptible to parameter variation within the limits set by the controller constants.[14–19] Detailed design associated with the controller and comparisons to two other controllers are discussed in References 18 and 19. In this paper the equations which calculate the frequency shift are quoted. At first, a sliding line is calculated by knowing the measured phase error, which is equal to

$$S(t) = \delta\Psi(t) + c\int \delta\Psi(t)dt \tag{10}$$

where c is the eigen value which is responsible for fixing the response time of the loop. A control function is obtained by monitoring the sign of the function $S(t)$,

given by

$$u(t) = -(k_1|\delta\Psi(t)| + k_0)\,\mathrm{sgn}\; S(t) \tag{11}$$

where $\mathrm{sgn}\, S(t)$ is $+1$ when $S(t)$ is positive and -1 when $S(t)$ is negative, and $|\delta\Psi(t)|$ is the absolute value of the phase error. Note that k_0 and k_1 are positive constants and must be set so as to make the loop stable and more robust. After this the frequency shift, $\delta f(t)$, is calculated from the following equation:

$$\delta f(t) = \frac{h}{2\pi}u(t) - \left(\frac{h}{2\pi}\right)^2 \frac{1}{f(t)} \left[\frac{\gamma(t)}{\gamma_T}\right]^2 u^2(t) \tag{12}$$

The coefficient of $u^2(t)$ is constant for a given MEB turn. These are stored in the DSP at each MEB turn or as many times as the corrections are needed. Values of the constants c, k_0 and k_1 are also stored in the DSP. The control functions satisfy the global stability of the loop by satisfying the conditions set by the Lyapunov Stability Theory. In Figure 6 the synchronizing phase error is plotted against time for $c = 2000$, $k_1 = 25$ and $k_0 = 0.5$ by assuming an initial phase error of 5 meters. It can be seen that the phase error becomes zero within the first 10 milliseconds. Loop response can be made slow by suitably selecting the controller constants. In Figures 7 and 8 the frequency shift, $\delta f(t)$, and the perturbed radial position are shown with respect to time.

5. PHASE MEASUREMENT

Equation 9 gives an indication of the system to be controlled. Using this system equation, the controller functions shown by Equations 10, 11 and 12 were obtained to correct for errors in the synchronizing phase. An accurate detection of the phase error is important to guarantee the controller operation. The phase error can be detected for one or two MEB turns, depending on the magnitude of the error.

Waiting much longer than one MEB turn to measure the LEB phase could lead to large error. The consequence will be greater frequency shift generated

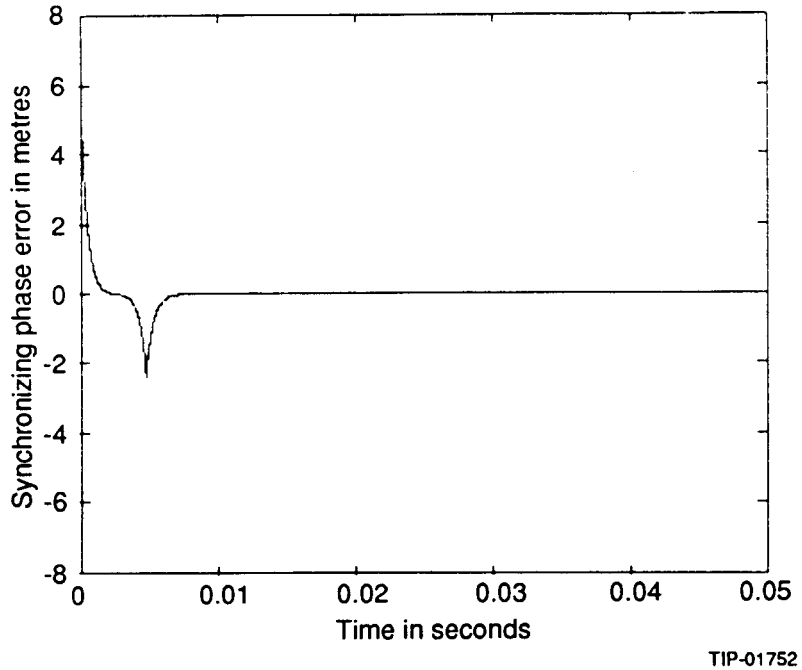

Figure 6. Decay of the synchronizing phase error, $\delta\Psi(t)$, as a function of time with the feedback loop closed.

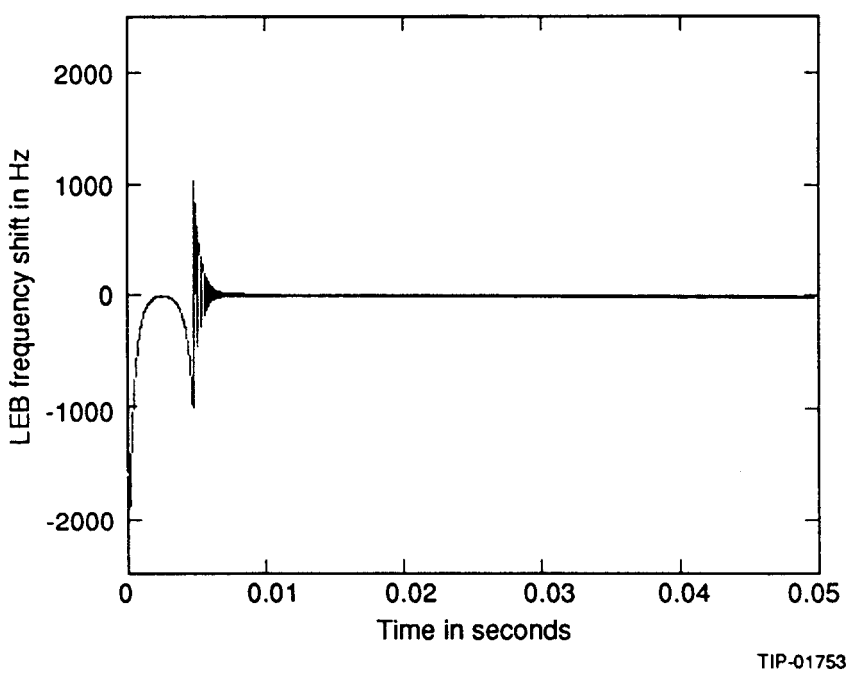

Figure 7. Decay of the frequency shift, $\delta f(t)$, as a function of time with the feedback loop closed.

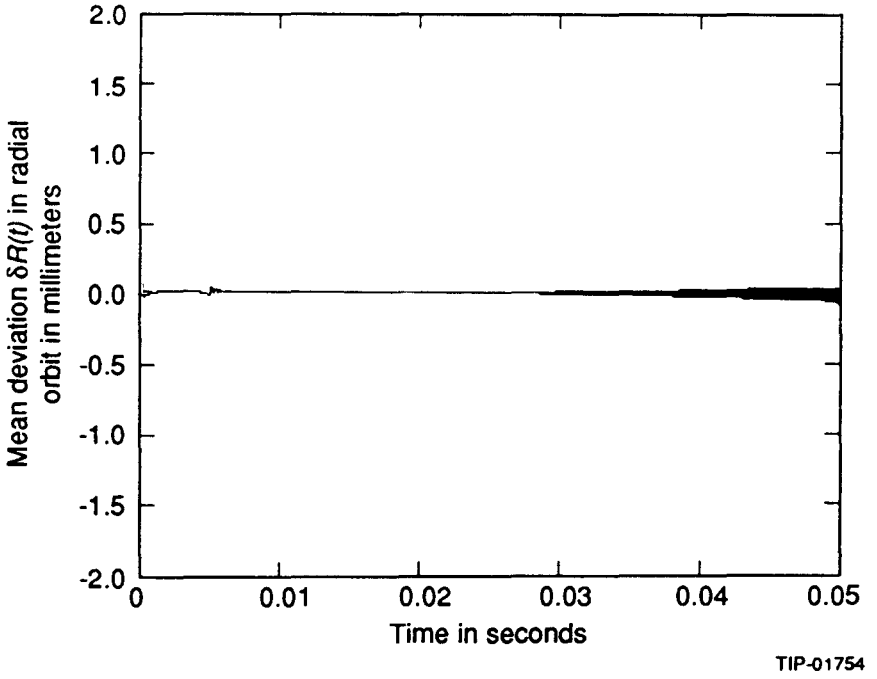

Figure 8. Perturbation on the mean deviation in the radial orbit as a function of time with the feedback loop closed.

by the feedback controller, which may lead to beam oscillations. The MEB completes about 3774 turns before it is ready to accept the beam from the LEB; if the phase is measured at every MEB turn, there will be 3774 points in the LEB cycle where the frequency shift has to take place. This is possible if the hardware can extract the phase error from the measured LEB phase and then solve Equations 10, 11 and 12 within the available time. One of the ways the LEB phase can be measured approximately is by time-tagging the arrival time of the LEB reference wave from the instant the MEB reference wave completes the turn. In the development system considered here, a Time to Digital Converter (TDC) will be used to record the arrival time of the LEB reference wave. Using this time of flight information, the phase of the LEB reference wave is calculated in terms of the path length by using the following equation:

$$\Psi'_{\text{measured}}(t) = 2\pi(R + \delta R(t))\,\frac{f(t) + \delta f(t)}{h}\,\tau' \tag{13}$$

where τ' is the arrival time of the LEB reference wave, $\delta f(t)$ is the frequency shift of the LEB frequency in the previous MEB turn, and $\delta R(t)$ is the average

radial position offset during the time-tagging period. Equation 13 assumes no frequency shift while measuring the arrival time of the LEB reference wave. The phase error is calculated by subtracting the measured LEB phase values from those shown in Figure 4 for a given MEB turn. This will be done inside the DSP in real time.

6. HARDWARE DESCRIPTION

The choice of hardware was driven by the need to demonstrate the basic principle established above to synchronize the variable frequency source of the LEB with the fixed frequency source of the MEB. Three stages of development are planned. The first stage will be to prove that the phase of the LEB can be controlled to the inexorable trip-plan to achieve synchronization at the designated MEB turn, in the absence of field errors. The second stage will be to insert errors in the B-field and study the effect of the control loop. In the third stage the feedback controller will be redesigned to include the radial position correction. When all three stages work together, the system will be delivering controlled master frequency to the accelerator cavities.

A schematic representation of the system block diagram for the first stage is shown in Figure 9. Two 32-bit floating point Digital Signal Processors, TMS320C30, from Texas Instruments were used as the processing units.[20,21] The configuration of the C30 DSP board, made by SKY Computers,[22,23] is shown in Figure 10. The DSP board has 2 Mb of Dynamic RAM and the usual control registers to interface to the VME bus. All the communication to the UNIX machine is done through the VME interface bus. The Node RAM in each C30 processor is a static memory and is 64 K words long. The first C30 is used to generate the master frequency by reading the frequency data stored in the SRAM, and then launching it to the LEB frequency synthesizer at the fine time intervals mentioned above. The MEB frequency synthesizer is running at the LEB extraction frequency. The counters, dividing by 108 and 792, represent the number of rf waves in one revolution in the LEB and the MEB, respectively. The

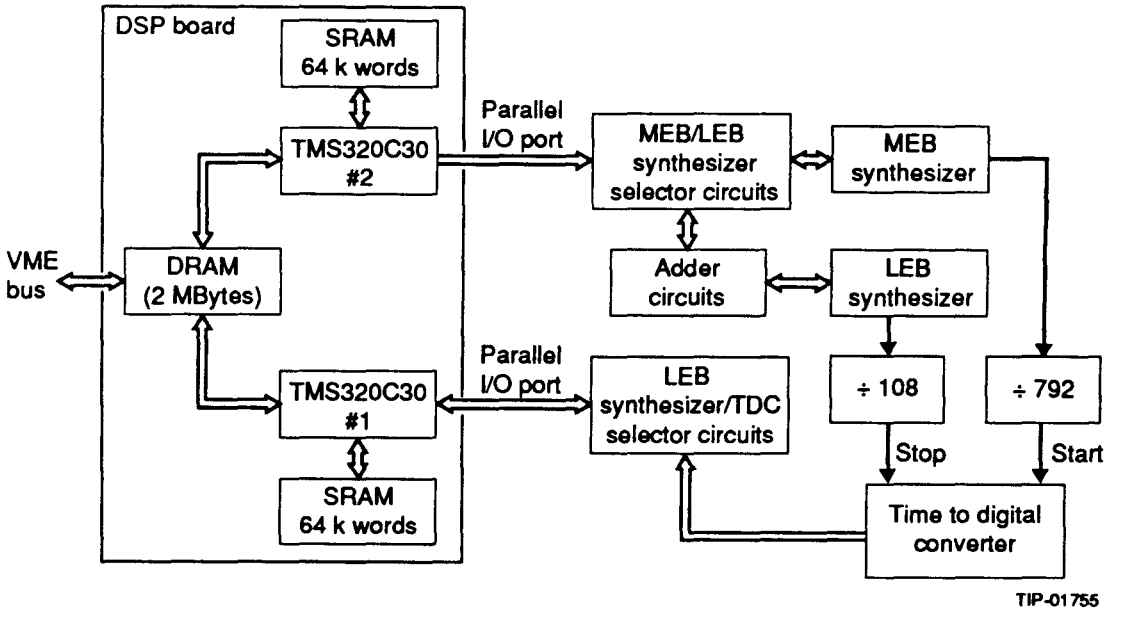

Figure 9. Schematic representation of the System Block Diagram.

TDC measures the arrival time of the first LEB reference pulse after every MEB reference pulse. The data is then read into the second C30 to solve Equations 10, 11, 12 and 13 by reading appropriate values from the global memory. The frequency shift $\delta f(t)$ is fed to the adder circuits to correct the master frequency. The operation of the feedback loop is repeated every MEB turn. The feedback loop must execute the following functions within one MEB turn, which is about 13.249 μs long.

(a) "Time of arrival" measurement using the TDC

(b) Handshaking between the TDC and the DSP for data acquisition

(c) LEB phase from Equation 13

(d) Phase error by subtracting the results of (c) from the trip-plan

(e) Frequency shift by solving Equations 10, 11 and 12

(f) Addition of the frequency shift with the master frequency

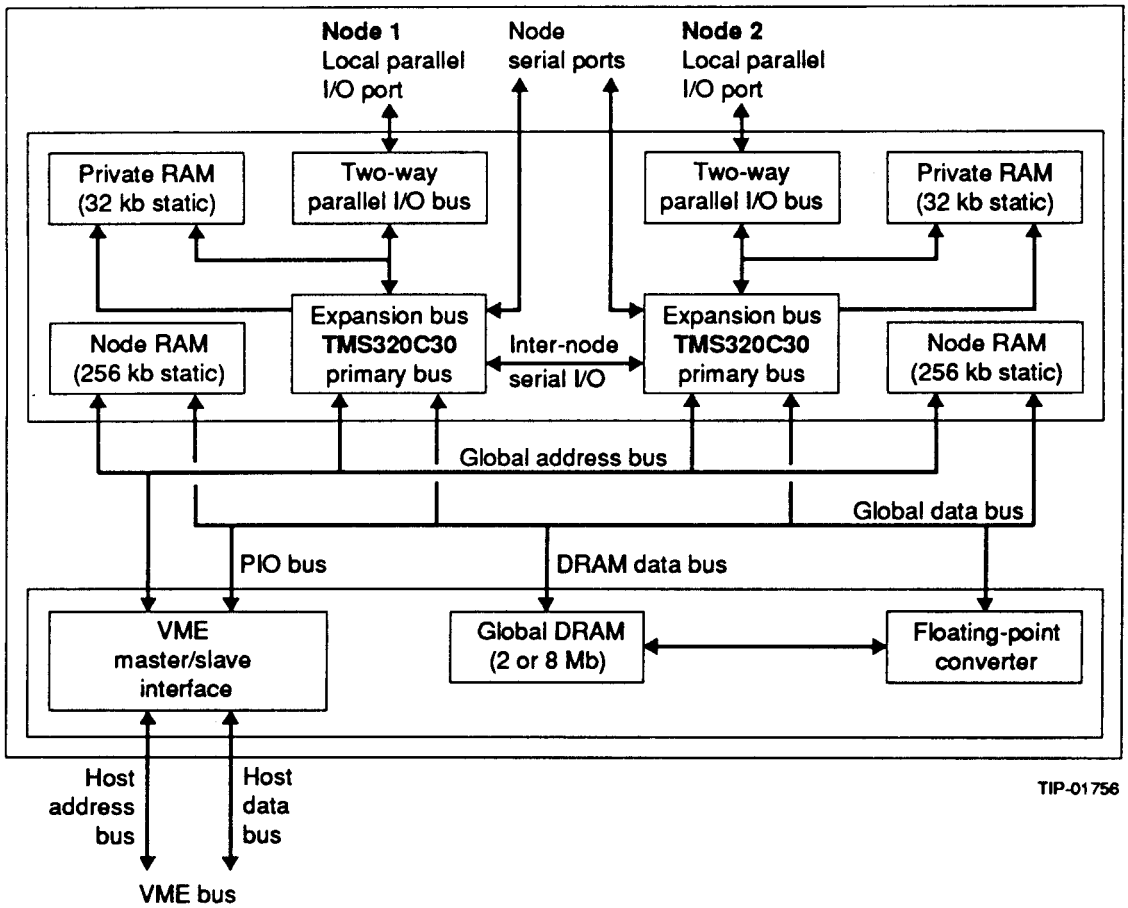

Figure 10. Schematic representation of the Internal Architecture of the DSP Board (Courtesy of SKY Computers).

Due to the simple control algorithm shown above and with the aid of a C30 processor, it is possible to compute all the functions within the available time.

7. CONCLUSIONS

In this paper the principle behind generating the controlled master frequency is shown. It is important to note at this stage that the benefit of this approach depends on how well the system works on the real accelerator. The greatest advantage of the control scheme is the ability to select any bunch in the LEB and then transfer to the MEB. This helps to include gaps in the LEB to prevent radiation on the extraction beam line due to finite kicker rise time. Current technology has provided Direct Digital Synthesizers which can sweep the LEB

frequency at more than a 5 MHz rate, combined with 32-bit frequency resolution and rf to 400 MHz. The phase discontinuity for all bit combinations must be tested before they can be used on the accelerator. From the feedback point of view it is believed that the DSP, TDC and DDS combination can produce the required control function. Also, since a DSP is used in the system, it will be easier to implement the control function when an additional feedback loop is needed to contain the transverse beam orbit within the specified limits.

8. ACKNOWLEDGEMENTS

Many people are involved in the development of this system. The author wishes to thank John Mangino and Jim Santana for their direct involvement in the engineering aspect of the project. The author thanks Richard Talman and Bob Webber for their insight and timely suggestions. Technical discussions with Professor Kai Yeung on the controller design are gratefully acknowledged.

REFERENCES

1. D.J. Martin et al., *Early Instrumentation Projects at the SSC*, International Industrial Symposium on the Super Collider (IISSC), Miami (USA), March 14–16, 1990.

2. W. Kriens, *HERA Synchronization—RF Frequency Control & Transfer Timing*, Notes, September 1990.

3. *Site-Specific Conceptual Design of the SSC*, SSCL-SR-1056, July 1990.

4. J.A. Dinkel et al., "Synchronous Transfer of Beam from the NAL Fast Cycling Booster Synchrotron to the NAL Main Ring System," *IEEE Transactions on Nuclear Science*, Vol. **NS-20**, No. 3, June 1973.

5. Y. Kimura et al., "Synchronous Transfer of Beam from the Booster to the Main Ring in the KEK Proton Synchrotron," *IEEE Transactions on Nuclear Science*, Vol. **NS-24,** No. 3, June 1977.

6. J.E. Griffin et al., private technical discussion, FNAL, Chicago, Illinois, February 1990.

7. J. Peterson and M. Furman, *Beam Synchronization & SSC Filling Time Considerations*, SSC Laboratory Report, SSCL-N-714, 1989.

8. S.R. Koscielniak, *RF Synchronization during Transfer of Batches from Booster to Collector*, TRIUMF Design Note, TRI-DN-89-K74, October 1989.

9. J.E. Griffin, "Heuristic Document on Phase-locking Scheme," unpublished, April 27, 1990.

10. M.T. Ronan et al., *Timing and RF Synchronization for Filling PEP/SPEAR with the SLC Damping Rings*, IEEE Particle Accelerator Conference, Chicago, Illinois, March 20–23, 1989.

11. L.C. Teng, *Matching and Synchronization during Transfer from Booster to Main Ring at 8 GeV*, FNAL Technical Note, TM-281, January 4, 1971.

12. L.C. Teng, *Synchronous Transfer of Beam from Main Ring to Energy Doubler*, FNAL Technical Note, TM-489, May 1, 1974.

13. G. Rees, private technical discussion, RAL, United Kingdom, December 1989.

14. U. Itkis, *Control Systems of Variable Structure*, John Wiley & Sons, New York, 1976.

15. V.I. Utkin, "Variable Structure Systems with Sliding Modes," *IEEE Transactions on Automatic Control*, Vol. **AC-22**, No. 2, April 1977.

16. P.K. Nandam and P.C. Sen, "A Comparative Study of a Luenberger Observer and Adaptive Observer-Based Variable Structure Speed Control System Using a Self-Controlled Synchronous Motor," *IEEE Transactions on Industrial Electronics*, Vol. **37**, No. 2, April 1990.

17. K.S. Yeung and Y.P. Chen, "A New Controller Design for Manipulators Using the Theory of Variable Structure Systems," *IEEE Transactions on Automatic Control*, Vol. **33**, No. 2, February 1988.

18. L.K. Mestha, *Phase-Control Scheme for Synchronous Beam Transfer from the Low Energy Booster to the Medium Energy Booster*, SSC Laboratory Report, SSCL-340, 1990.

19. L.K. Mestha et al., "Synchronization of Variable Frequency Source with a Fixed Frequency Source Using Sliding-Mode Controller," to be published in the *IEEE Particle Accelerator Conference*, San Francisco, May 6–9, 1991.

20. *TMS320C3X User's Guide*, Texas Instruments, SPRU031A, USA, 1990.

21. *Digital Signal Processing Applications with the TMS320 Family, Theory, Algorithms, and Implementations*, Texas Instruments, Vol. **3**, SPRA017, USA, 1990.

22. *Challenger-C30 Programmer's Guide*, SKY Computers, CHC30-VME-PG-90-1.0, Chelmsford, Massachusetts, May 29, 1990.

23. *Challenger-C30 Hardware Reference Manual*, SKY Computers, CHC30-VME-HR-90-1.0, Chelmsford, Massachusetts, May 31, 1990.